Noncontact evaluation of the conductivity of CuPc thin films by near-field microwave microprobe method

Lkhamsuren Enkhtur[a], Ragchaa Galbadrakh[a], Tigran Sargsyan[b], Harutyun Melikyan[b], Arsen Babajanyan[b], Barry Friedman[c], Kiejin Lee[b,*]

[a] *Department of Theoretical and Experimental Physics, National University of Mongolia ,Ulaanbaatar, Mongolia*
[b] *Department of Physics and Interdisciplinary Program of Integrated Biotechnology,Sogang University, Seoul 121-742, Korea*
[c] *Department of Physics, Sam Houston State University, Huntsville, Texas 77341, USA*

Abstract

The conductivity of copper II phthalocyanine (CuPc) thin films with different crystal structures and morphologies was evaluated by using a near-field microwave microprobe (NFMM) technique in the frequency range of 4-4.5 GHz. CuPc thin films annealed at 200 °C and 350 °C showed the α- and β-phase crystal structures, respectively. Crystal phase structure and morphology of CuPc thin films were characterized by optical absorption spectra measurement, X-ray diffraction, and scanning electron microscopy methods. Conductivity measurements of CuPc thin films were done in the temperatures range of 25 - 160 °C.

PACS: 68.37.-d; 68.37.Uv; 68.55.-a; 68.60.-p
Keywords: CuPc; annealing; conductivity, intrinsic impedance; near-field; microwave microprobe
*Corresponding author. Tel.: +82 2 705 8429; fax: +82 2 715 8429.
E-mail address: klee@sogang.ac.kr (K. Lee).

1. INTRODUCTION

Copper phthalocyanine (CuPc) is one of the promising organic compounds due to its low cost, high thermal and chemical stability, and its excellent field effect response [1-2]. Organic field effect transistors (OFETs) have attracted much attention because of their potential applications in organic/molecular electronics. Much research effort was being dedicated to improvement of characteristics of OFETs composed of CuPc thin film [3-10]. Intrinsic properties of CuPc thin film such as crystal structure, microstructure of grains, band gap and thickness influence the characteristics of OFET device. In this paper we have investigated the annealing effect on CuPc thin film conductivity. As the substrate annealing temperature increased, the conductivity of CuPc thin films was changed. The conductivity of CuPc thin films was estimated by a noncontact near-field microwave microprobe method. Near-field microwave microprobe (NFMM) techniques with high sensitivity have been developed for the characterization of thin films from the microwave to the millimeter-wave ranges [11-16]. An important ability of the NFMM is contactless characterization of thin films, in particular, the characterization of electrical properties of thin films, such as conductivity, resistivity, and dielectric permeability. Contactless and nondestructive characterization techniques are very useful for the device applications of organic devices. The NFMM technique, which directly measures the physical properties such as surface conductivity of thin films, shows practical promise. We have used a NFMM coupled to a high-quality dielectric resonator with a distance regulation system at an operating frequency $f = 4$ - 4.5 GHz. The conductivity changes of CuPc films due to the different annealing temperatures were investigated using a NFMM by measuring the microwave reflection coefficient S_{11}.

2. THEORY

The charge transport properties in organic semiconductors are quite different from those in inorganic materials and thus this issue has attracted a great deal interest in CuPc. We have therefore conducted high-sensitivity dielectric measurements in CuPc thin films prepared under different annealing conditions. In generally, the complex dielectric permittivity of CuPc thin films is a function of frequency ($\omega = 2\pi f$) and temperature (T):

$$\varepsilon(\omega,T) = \varepsilon'(\omega,T) - j\varepsilon''(\omega,T), \qquad (1)$$

where ε' and ε'' are the real and the imaginary parts of the complex dielectric permittivity. The conductivity is related to ε'' by

$$\varepsilon''(\omega,T) = \frac{\sigma(\omega,T)}{\omega\varepsilon_0}, \qquad (2)$$

where ε_0 is the dielectric permittivity of the vacuum. We explore the conducting properties of CuPc thin films in the frequency range of 4 - 4.5 GHz by measuring the microwave reflection coefficient. The propagating electromagnetic wave at standing-wave regime is derived from the Maxwell equations as [17]

$$V(z) = V_0^+ e^{-jk_s z} + V_0^- e^{jk_s z}, \qquad (3)$$

where the first and the second parts in Eq. (3) are the incident (generated from microwave source) and reflected (from sample) waves, respectively. The voltage complex reflection coefficient in logarithmical scale (S parameter) at the semiconductor interface can be derived by using standard transmission line theory and is given by assuming impedance matching between the microwave probe and the microwave source [17]

$$S_{11} = 20\log\left|\frac{Z_c - Z_0}{Z_c + Z_0}\right|, \qquad (4)$$

where Z_0 is the characteristic impedance of probe with the fixed value of Z_0 = 50 Ω, Z_c is the complex intrinsic impedance of the CuPc thin film, and it can be estimate as [17]

$$Z_c = \frac{Z_a}{\sqrt{\varepsilon_c(\omega)}}, \qquad (5)$$

where Z_a is the impedance of air (Z_a = 377 Ω) and ε_c is the complex dielectric permittivity of CuPc. After some algebra, the complex intrinsic impedance of CuPc thin film can be expressed as

$$Z_c = \frac{Z_a}{\sqrt{\varepsilon_c'}} \cdot \left[\frac{1+\sigma_c^2/(8\omega^2\varepsilon_c'^2)}{1+\sigma_c^2/(2\omega^2\varepsilon_c'^2)} + j\frac{\sigma_c/(2\omega\varepsilon_c')}{1+\sigma_c^2/(2\omega^2\varepsilon_c'^2)}\right], \qquad (6)$$

where σ_c, and ε_c' are the conductivity and the real part of the complex permittivity of the CuPc thin film.

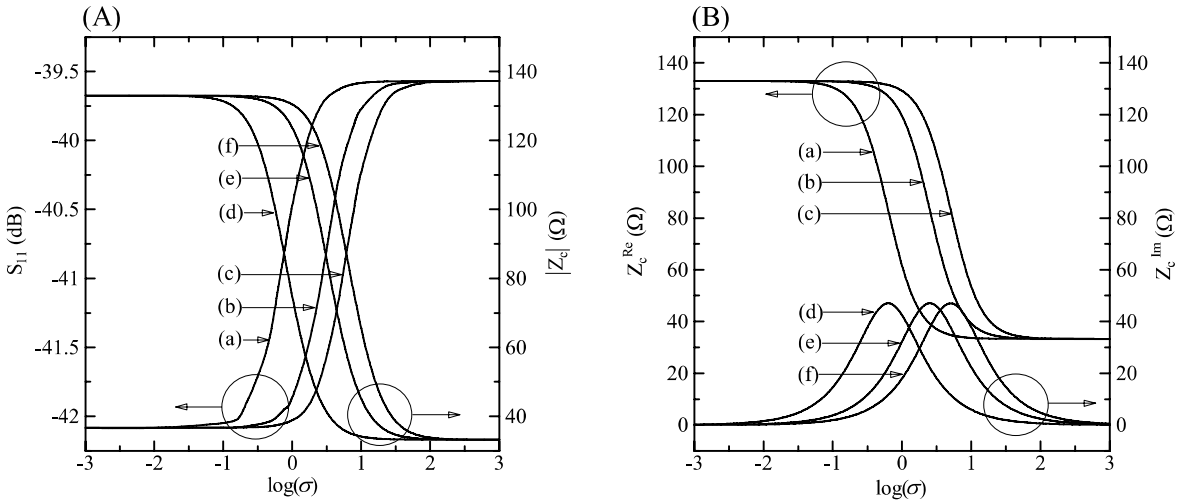

Figure 1. (A) The calculated reflection coefficient (left axis) and sample intrinsic impedance magnitude (right axis) of CuPc sample as a function of sample conductivity on a log scale at (a); (d) 1 GHz, (b); (e) 4 GHz, and (c); (f) 8 GHz. (B) The CuPc sample complex intrinsic impedance real (left axis) and imaginary (right axis) parts dependences on CuPc thin film conductivity on a log scale at (a); (d) 1 GHz, (b); (e) 4 GHz, and (c); (f) 8 GHz.

Figure 1 (A) shows the calculated reflection coefficient (left axis) and the magnitude of intrinsic impedance (right axis) of CuPc thin films as a function of sample conductivity with different three microwave frequencies as a parameter. The microwave frequencies varied from 1 to 8 GHz. At the low conductivity range, the reflectance became flat for each frequency and equal to the Fresnel value for an insulator. At the high conductivity limit, the reflectance approached metallic behavior. Figure 1 (B) shows the complex intrinsic impedance Z_c. Real (left axis) and imaginary (right axis) parts are shown as a function of conductivity on a log scale. Note, that $Real\{Z_c\} >> Im\{Z_c\}$, so the real part can be estimated from the total complex intrinsic impedance of CuPc thin films.

2. EXPERIMENT

2.1. Sample preparation

CuPc powder was purchased from Aldrich Chemical Co. and used without further

purification. Slide glass was used as a substrate. The substrate was cleaned with acetone, ethyl alcohol and distilled water. The CuPc thin films are fabricated by the standard vacuum evaporation technique. A Cu-Pc source, contained in a ceramic crucible, was resistively heated in high vacuum chamber at 10^{-7} Torr. The deposition rate was controlled at 0.02 - 0.05 nm/sec. The resulting films were about 100 nm thick with deposition rate and thickness monitored by a thickness monitor. During deposition substrate temperature was 25 °C (room temperature). In order to study the effect of annealing three samples were prepared: as deposited thin film and films annealed at 200 °C and 350 °C for 1 hour. For conductivity measurements gold contacts were deposited on the surface of the CuPc thin films with a thickness of 300 nm and a channel length of 50 μm.

2.2. Experimental setup

The optical absorption of the CuPc thin films was measured in the range 450-850 nm using a SCINCO UV-Vis spectrometer. The change of the crystal structure of CuPc thin films was inspected by x-ray diffraction. Surface morphology of the films was characterized by a scanning electron microscope (SEM). The temperature dependence of conductivity of thin films was measured by a source meter (Keithley 2400) and the conductivity of the thin films was estimated by the measurement with a NFMM. The experimental setup of our NFMM was described in detail in Ref. [13]. We designed a NFMM system with a tuning fork distance control system to keep a constant distance between the sample and the tip. The probe tip was made of gold wire with a diameter of 50 μm with tapered end size of 1 μm. The probe tip was oriented perpendicular to the sample surface and the other end of the tip was directly connected to a coupling loop in the dielectric resonator. The reflection coefficient S_{11} was measured by network analyzer (Agilent 8722ES). To drive the tuning fork, an AC voltage was applied to one contact on the tuning fork at its resonance frequency using the oscillator of a lock-in amplifier. The resulting current from the other contact was measured by using the current input of the same lock-in amplifier. The output from the lock-in amplifier was fed into the feedback system to control the tip-sample distance using a piezo electric tube (PZT) that supports the sample stage. The probe tip to sample distance was kept at about 10 nm. All NSMM measurements were made at the same sample-tip distance. The sample was mounted onto an x-y-z-translation stage for coarse adjustment which was driven by a computer-controlled microstepping motor with a resolution of 0.01 μm, whereas fine movement of the sample was controlled by a PZT tube.

4. RESULTS AND DISCUSSION

The absorption spectra of CuPc thin films depends on the crystal structure [18,19]. The α-phase of CuPc thin films shows the two absorption maxima located at wavelength of 625 and 694 nm while the β-phase shows two maxima located at wavelength of 645 and 720 nm [20].

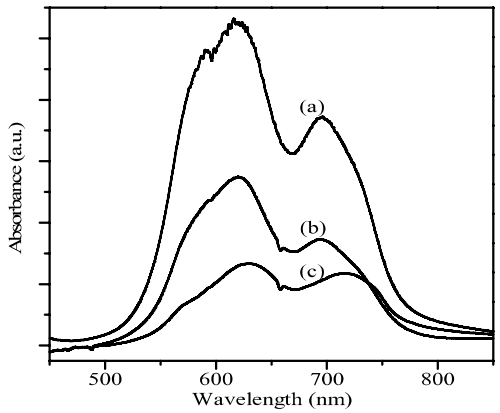

Figure 2. Optical absorption spectra of CuPc thin films (a) RT sample, (b) annealed at 200 °C and (c) annealed at 350 °C.

Figure 2 shows the optical absorption spectra of CuPc thin films deposited at room temperature and annealed at different temperatures for 1 hour. As shown in Fig. 2, for the absorption spectra of the as-deposited thin film (RT) the higher energy maximum peak is larger than that of the second peak. Similar behavior is shown by the thin film annealed at 200 °C. This behavior represents the typical features of the α-phase of CuPc thin films. As the annealing temperature increased to 350 °C, the peak positions were changed to the maximum peaks positions of the β-phase of CuPc [21,22]. The positions of the absorption peaks and

the related values of the direct energy gap are given in Table 1.

Table 1. Positions of absorption peak and the direct energy gap of CuPc deposited on glass and annealed at different temperatures.

Annealing temperature (°C)	Position of absorption peaks (nm)		Direct energy gap (eV)	
	1st peak	2nd peak	1st peak	2nd peak
25 (RT)	611.4	695.8	2.03	1.78
200	619.8	693.5	2.00	1.79
350	629.3	715.4	1.97	1.73

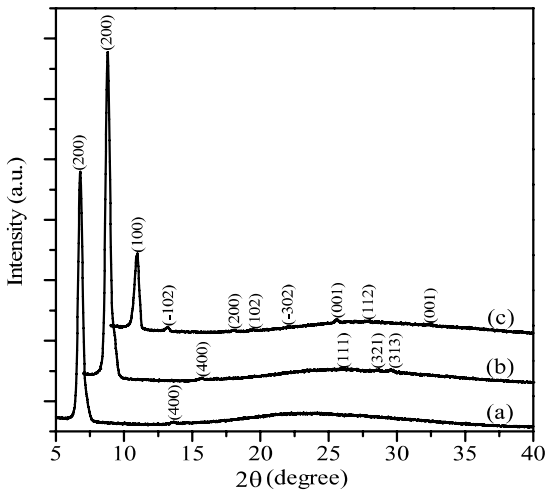

Figure 3. X-ray diffraction spectra of CuPc thin films (a) RT sample, (b) annealed at 200 ℃ and (c) annealed at 350 ℃.

Figure 3 shows the x-ray diffraction patterns for Cu-Pc thin films annealed at different temperatures. CuPc thin films deposited at room temperature showed two distinct peaks at 6.7° and 13.5°, corresponding to the (002) and (400) lattice plane of the α-phase of CuPc. At the annealing temperature of 200 °C, five peaks corresponding to the crystal structure of the α-phase of CuPc were observed. CuPc thin films annealed at 350 °C showed the distinct eight peaks corresponding to the β-phase. The calculated crystal cell parameters were $a = 1.464$ nm, $b = 0.470$ nm, $c = 1.732$ nm, $\alpha = 90.00$ °, $\beta = 105.49$ °, and $\gamma = 90.00$ °. The space group of the crystal structure was monoclinic $P2_1/c$ and agreed well with Ref. [23]. By annealing at 270 °C, we obtained the mixture structure of α- and β-phases.

Figure 4 shows the SEM images of CuPc thin films deposited (a) at room temperature, (b) annealed at 200 °C, and (c) 350 °C. At room temperature, randomly oriented nanorods were observed. The shapes of cross sections of the nanorods are rectangular. As the annealing temperature increased to 200 °C, the nanorods merged standing up perpendicularly to the substrate surface. For the annealing temperature of 350°C, the nanorods have a horizontally periodic lamellar shape with the ends some being whiskers-like (see Fig. 4 (c)).

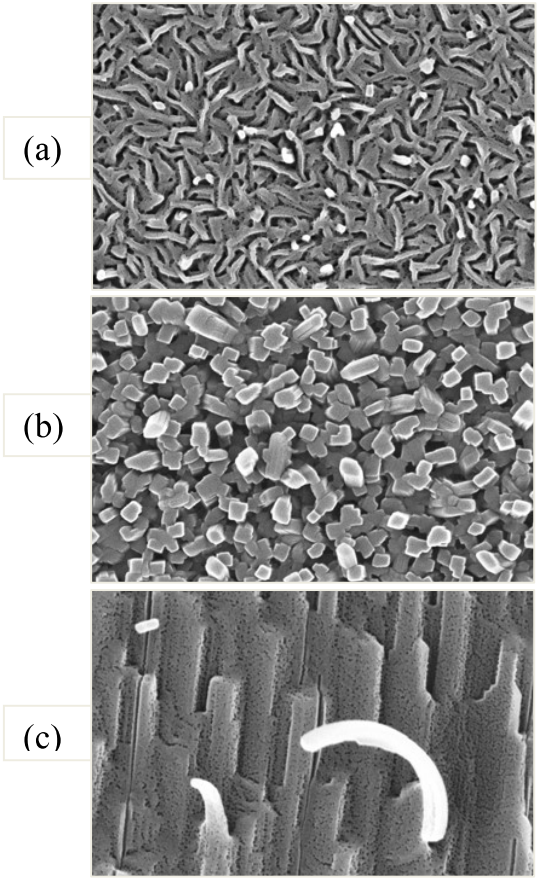

Figure 4. SEM images of CuPc thin films (a) RT sample, (b) annealed at 200 ℃ and (c) annealed at 350 ℃.

It is noticeable that the grain orientation and the crystal structure of CuPc thin films were drastically changed above 300 °C of annealing temperature. To our knowledge, this has not been previously observed.

The transport properties of CuPc thin films depend on the crystal structure, energy band structure, and grain morphologies [21]. The conductivity of CuPc thin film at room temperature has an order of magnitude of 10^{-10} S/m [24]. In a practical situation the conductivity and the mobility measurement of CuPc thin films is evaluated by using a field effect transistor. Here voltage and current were measured for the temperature range from 25 to 160 °C by a two probe method.

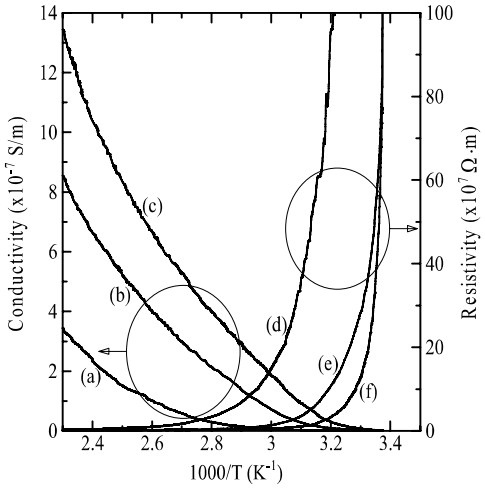

Figure 5. The conductivity (left axis) and resistivity (right axis) of CuPc thin films as a function of measurement temperature for (a); (d) RT sample and annealed at (b); (e) 200 °C and (c); (f) 350 °C temperatures.

Figure 5 shows the conductivity (left axis) and the resistivity (right axis) of CuPc thin films annealed at different temperatures as the function of temperatures. The conductivity of CuPc thin films annealed at 350 °C, which has the β-phase, shows higher conductivity than that of films annealed at 200 °C, which has a α-phase. These shows that the conductivity of CuPc thin film increased as the annealing temperature increase up to 350°C, as the crystal structure changed from α-phase to the β-phase. From temperature-conductivity dependencies in the temperature range of 25 - 50 °C, using an Arrhenius' plot, we could estimate the thermal activation energy. In an Arrhenius' plot we represent the electrical conductivity temperature dependence by the expression: $\sigma = \sigma_0 \exp(-E_a / 2kT)$, where E_a is the thermal activation energy, k is the Boltzmann constant, T is the absolute temperature, and σ_0 is the initial conductivity of CuPc. Calculated values of thermal activation energy of CuPc thin films at room temperature, annealed at 200 °C, and 350 °C were (a) 1.88 eV, (b) 1.84 eV, and (c) 1.80 eV, respectively. The direct band gap energy from absorption spectra gives similar through somewhat smaller values (see Table 1). Note that, the thermal activation energy of CuPc thin film deposited on ITO substrates which was measured by the field effect method (1.49 eV [25]) was close to the band gap energy (1.59 eV) defined by photoelectron emission and by optical absorption [26]. A study of transport properties of CuPc thin films deposited on ITO glass and annealed at different temperatures used an ITO bottom contact and an Au electrode evaporated on top of the sample [21]. Due to heating of the thin film substrate from RT to 350 °C the energy gap was changed from 1.8052 to 1.7844 eV [21]. These values are close to our measured thermal activation energy of CuPc thin films deposited on the glass substrate. Consequently, as the crystal structure changed from α-phase to β-phase the conductivity of CuPc thin film was increased.

Figure 6 (A) shows the measured microwave reflection coefficient S_{11} profile of CuPc thin films (a) without sample, annealed at (b) RT, (c) 200 °C, and (d) 350 °C for 1 hour. The matched resonant curve of the air has a minimum level of -52.09 dB, which is the reference level of S_{11} of our measurements. As the annealing temperatures increased up to 350 °C, the minimum reflection coefficient S_{11} increased from -42.09 dB to -39.24 dB, as shown in the inset to Fig. 6 (A). The change of reflection coefficient depended on the conductivity of CuPc thin films. Note, that 100 nm CuPc thin film conductivity was about 10^{-10} S/m for as-growth thin films [18]. The reflection coefficient S_{11} increased as the annealing temperature increased up to up to 350 °C. The changes of reflection coefficient S_{11} depends on variations of the conductivity of CuPc thin film as we can see from Eq. (4) and (6). Comparing to RT, the conductivity of CuPc thin film increased about 83 times for 200 °C and 100 times at the 350 °C annealing. Figure 6 (B) shows the estimated conductivity of CuPc thin films (left axis) and the resistivity (right axis) as a function of annealing temperatures. As the annealing temperatures increased up to 350 °C, the conductivity increased from 10^{-10} to 10^{-8} S/m. Therefore our results obtained by NFMM method well agree with results measured by field effect measurements [25].

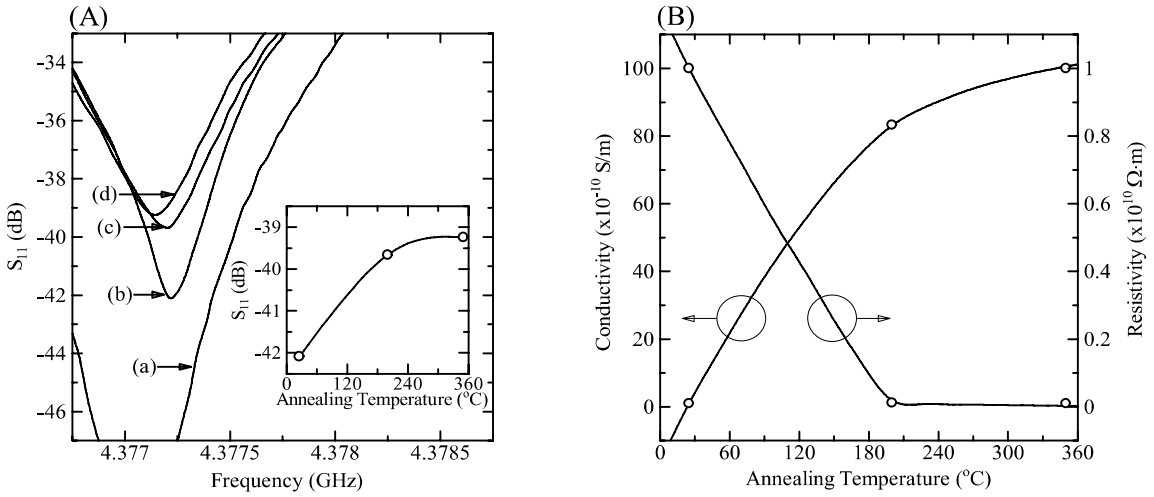

Figure 6. (A) The microwave reflection coefficient S_{11} profile for (a) air and CuPc thin films for (b) RT sample and annealed at (c) 200 ℃ and (d) 350 ℃. (B) Estimated CuPc thin film conductivity (left axis) and resistivity (left axis) as a function on sample annealing temperature. Solid line is the guide for the eye.

5. SUMMARY

The annealing procedure at different temperatures changes the crystal phase structure and grain microstructure of CuPc thin films. By annealing at 350 °C the β-phase CuPc thin film is obtained on the glass substrate. Annealing procedure at 350 °C increases conductivity of CuPc thin film evaporated at room temperature up to 100 times and decreases thermal activation energy by 0.08 eV. The NFMM method is useful for the measurement of the electrical properties of organic thin films.

ACKNOWLEDGMENTS

This work was supported by Sogang University (2007), by Korean Foundation for Advanced Studies, by the Korea Research Foundation (KRF-2005-042-C00058; KRF-2002-005-CS0003), Seoul Research and Business Development Program (10816) and by the Korea Science & Engineering Foundation (F01-2004-000-1082-0; R01-2006-000-11227-0), by Korean Foundation for Advanced Studies- International Scholar Exchange Fellowship for academic year 2007-2008, by projects H.1.7.2 and H.2.6.2 within the Innovation Development program of Mongolian Government.

REFERENCES

[1] J. Simon, J. Andre, Molecular Semiconductors, Springer, Berlin, 1985.

[2] C. Leznoff, A. Lever, Phthlocyanines: Properties and Applications, VCH, New York, 1993.

[3] Zh. Bao, A. Lovinger, A. Dodabaladur, Appl.Phys. Lett. 69 (1996) 3066.

[4] M. Gorgoi, D. Zahn, App. Surf. Science 252 (2006) 5453.

[5] J. Puigdollers, C. Voz, M. Fonrodona, S. Cheylan, M. Stella, J. Andreu, M.Vetter, R.Alcubilla, J. Non-Cryst. Solids 352 (2006) 1778.

[6] T. Yasuda, T. Tsutsui, Chem. Phys. Lett. 402 (2005) 395.

[7] S. Hoshino, T. Kamada, K. Yase, J. Appl. Phys. 92 (2002) 6028.

[8] K. Xiao, Y. Liu, G. Yu, D. Zhu, Synth. Met. 137 (2003) 991.

[9] V. Aristov, O. Molodtsova, V. Maslyuk, D. Vyalikh, V. Zhilin, Yu. Ossipyan, T. Bredow, I. Mertig, M. Knupfer, App. Surf. Science 254 (2007) 20.

[10] K. Xiao, Y. Liu, G. Yu, D. Zhu, Appl. Phys. A 77 (2003) 367.

[11] S. Dutta, C. Vlahacos, D. Steinhauer, A. Thanawalla, B. Feenstra, F. Wellstood, S. Anlage, H. Newman, Appl. Phys. Lett. 74 (1999) 156.

[12] B. Knoll, F. Keilmann, A. Kramer, R. Guckenberger, Appl. Phys. Lett. 70 (1997) 2667.

[13] J. Kim, M. Kim, H. Kim, D. Song, K. Lee, B. Friedman, Appl. Phys. Lett. 83 (2003) 1026.

[14] B. Friedman, M. Gaspar, S. Kalachikov, K. Lee, R. Levisky, G. Shen, H. Yoo, J. Am. Chem. Soc. 127 (2005) 9666.

[15] B. Friedman, B. Oetiker, K. Lee, J. Kor. Phys. Soc. 52 (2008) 588.

[16] M. Park, H. Yoo, S.Yun, E. Lim, K.Lee, Ch.

Chang, M. Joo, I. Lee, J. Kim, B. Friedman. App. Surf. Science 233 (2004) 213.

[17] D. Pozar, Microwave Engineering, Anderson-Wesley, New York, 1990.

[18] A. Djurisic, C. Kwong T. Lau,W. Guo, E. Li, Z. Liu, H. Kwok, L. Lam, W. Chan. Opt. Commun. 205 (2002) 155.

[19] H. Xia, M. Nogami. Opt. Mater. 15 (2000) 93.

[20] M. Barett, Z. Borkowska, M. Humphreys, R. Parsons, Thin Solid Films 28 (1975) 289.

[21] E. Jungyoon, S. Kim, E. Lim, K. Lee, D. Cha, B. Friedman, Appl. Surf. Sci. 205 (2003) 274.

[22] S. Karan, B. Malik, Solid State Commun. 143 (2007) 289.

[23] O. Berger, W. Fisher, B. Adolph, S. Tierbach, V. Melev, J. Sheirer, J. Mater. Sci. 11 (2000) 331.

[24] Ts. Sumimoto, M. Izuka, Sh. Kynioshi, K. Kudo, K. Tanaka, Y. Yu. J. Korean Phys. Soc. 31 (1997) 522.

[25] A. Ikushima, T. Kanno, Sh. Yoshida, A. Maeda, Thin Solid Films 273 (1996) 35.

[26] K. Kudo, Ts. Sumimoto, K. Hiraga, Sh. Kuniyoshi, K. Tanaka. Jpn. Appl. Phys. 36 (1997) 6994.